Journal of Artificial Intelligence in Medical Applications (JAIMA)
Vol. 1, No. 1, 2025, **pp.** 1–14
ISSN: 3106-1494 | **DOI**: https://doi.org/10.65511/jaima.v1i1.734

Efficient Blood Cell Classification Using a Hybrid Variational Quantum Circuit–EfficientNet Model on BloodMNIST

Eman A. Radhi [1], Mazin Abed Mohammed [2] *, Fatma Eid [3,4], Isabel de la Torre Díez [5]

[1]College of Science, Mustansiriyah University, Baghdad, Iraq; eman.a.r@uomustansiriyah.edu.iq
[2]Department of Artificial Intelligence, College of Computer Science and Information Technology, University of Anbar, Anbar 31001, Iraq; mazinalshujeary@uoanbar.edu.iq
[3]Department of Technology Management, College of Engineering and Applied Sciences, Stony Brook University, New York 11794, USA ; Fatma.eid@alumni.stonybrook.edu
[4]Department of Applied Artificial Intelligence, College of Computing and Informatics, Sungkyunkwan University, Seoul 03063, South Korea
[5]Departament of Signal, Theory and Communications. University of Valladolid, Spain; isator@uva.es

Received: 15/05/2025, Revised: 25/06/2025, Accepted: 07/07/2025, Published: 16/09/2025

ABSTRACT: Accurate classification of blood cells is crucial for early diagnosis and monitoring of hematological disorders. However, manual microscopy is time-consuming, subjective, and prone to inter-observer variability. Deep learning has shown potential in automating this task, but its high computational demands limit its use in resource-constrained settings. This study aims to develop an efficient, hybrid quantum-classical model for blood cell classification using quantum simulation to reduce computational complexity without compromising accuracy. We propose a hybrid framework that integrates a 6-qubit variational quantum circuit (VQC) with a classical EfficientNet-B0 model. The model was trained and tested on the full BloodMNIST dataset, which includes 17,092 microscopic images across eight blood cell types. The proposed model achieved a test accuracy of 96.58% and a validation accuracy of 96.90%. F1-scores ranged from 91.97% to 99.84%, with notable results in neutrophils (98.80%) and lymphocytes (98.36%). These findings confirm the feasibility of combining quantum and classical approaches for medical image classification. The proposed hybrid model shows strong promise for practical use in diagnostic systems, especially in low-resource settings, and offers a pathway for future research in quantum-enhanced medical imaging.

Keywords: Blood cell classification, Quantum machine learning, hybrid quantum-classical neural networks, variational quantum circuits, medical image analysis, hematology.

1. INTRODUCTION

Blood offers a crucial diagnostic window to human health, consisting of characteristic cellular components providing essential information regarding physiological state and disease processes. Human blood consists of three major cellular components: erythrocytes (red blood cells) that transport oxygen, leukocytes (white blood cells) which comprise the cellular defense of the immune system, and thrombocytes (platelets) which are irreplaceable for hemostasis and clotting [1, 2]. CBC (Complete Blood Count) analysis, which quantitates and characterizes these cellular populations, constitutes the most requested diagnostic test in clinical medicine, providing crucial information towards diagnosing conditions like anemia, infections, hematologic malignancies, and immune system disorders [3]. Modern automated hematological analyzers can evaluate as many as 120 samples per hour, providing accurate cell counts and differential leukocyte analysis with high throughput and reliability. However, when automated systems detect abnormal values or outliers, manual morphological examination using optical microscopy becomes essential for accurate differential diagnosis and clinical decision-making [4].

Morphological investigation of blood cells, particularly white blood cells, is a pillar of hematological diagnosis. White blood cells comprise a variety of subtypes, distinguished by characteristic morphological features and specific immune functions [5]: neutrophils represent the body's initial barrier to bacterial invasion, lymphocytes organize adaptive immune responses, monocytes serve as tissue macrophages, eosinophils respond to parasitic invasion and allergic processes, and basophils participate in inflammatory processes. Detailed identification and quantitation of these cellular types enable clinicians to assess immune apparatus function, detect infections, make blood cancer diagnoses, and monitor therapeutic response [6, 7]. Nonetheless, even following significant advances in automated hematology analyzers, manual microscopic inspection by skilled hematologists and lab technicians remains the standard for complex cases and definitive identification. The methodology comprises staining blood films with Romanowsky-type stains and systematic enumeration and classification of cells at high magnification [8]. Traditional blood cell classification technologies rely upon labor-intensive and time-consuming microscopy-based methods. These conventional approaches are often operator-dependent, resulting in inconsistent outcomes among different observers and variable results. Furthermore, these classification methodologies are not capable of handling sizeable databases, and hence, they are ineffective for high-throughput clinical applications as well as large-scale screening programs. Additionally, shortages of qualified personnel and advanced laboratory facilities in resource-limited settings constrain the scalability and reproducibility of traditional microscopy-based classification methods. These limitations highlight the urgent need for automated, accurate, and cost-effective technologies to support hematological monitoring and diagnosis [9].

The incorporation of artificial intelligence, particularly deep learning strategies, in medical imaging has shown great promise for automating blood cell analysis. Convolutional neural networks have demonstrated the capability to classify and identify various blood cell types from microscopic images, offering potential alternatives to the limitations of manual interpretation [10]. AI-based systems can process large image datasets consistently and efficiently, reduce analysis time, and may enhance diagnostic accuracy by detecting subtle morphological features that would go unnoticed by human observers [11]. Recent advances in deep learning-based blood cell classification have achieved substantial performance improvements. Advanced CNN architectures, such as ResNet, EfficientNet, and Vision Transformers, have been successfully employed across various blood cell datasets, yielding high classification accuracies and demonstrating robust performance across different cell types [12, 13]. These approaches have demonstrated certain effectiveness in handling deep morphological variation at the cellular level and distinguishing closely related cellular subtypes [14]. However, classical machine learning algorithms reach computational and performance ceilings in their application to complex medical imaging tasks. Deep neural networks are computationally demanding, require large sets of annotated data, and are extremely slow to train for optimal performance [15, 16]. Additionally, the "black box" nature of deep learning architectures can be a barrier to adoption among medical experts due to the requirement for explainable diagnostic systems to facilitate responsible clinical decision-making [17, 18]. These limitations have motivated exploration of alternative computational paradigms that can deliver advantages in efficiency, interpretability, or performance.

In healthcare applications, quantum computing has shown potential across multiple domains including drug discovery, genomics analysis, and medical imaging [19]. For medical imaging specifically, quantum-enhanced algorithms have been proposed for image reconstruction, pattern recognition, and feature extraction tasks [15, 20, 21]. Quantum machine learning, or QML, represents a uniquely promising point of contact between quantum computation and machine intelligence. QML algorithms leverage quantum computational abilities to possibly enhance classical machine learning workflows [22]. Theoretical analyses suggest that quantum algorithms can achieve exponential speedups for certain machine learning problems, particularly those featuring high-dimensional feature spaces typical of medical imaging applications [23]. Variational quantum circuits (VQCs) represent a practical means of implementing quantum machine learning algorithms on current noisy intermediate-scale quantum (NISQ) devices. VQCs consist of parameterized quantum gates whose parameters can be optimized using classical optimization techniques, similar to neural network training. This hybrid quantum-classical approach enables practical implementation of quantum algorithms while working within the constraints of modern quantum hardware limitations [24, 25]. The VQC architecture provides sufficient versatility for diverse machine learning applications. A typical VQC consists of data encoding circuits that convert classical data into quantum states, parameterized ansatz circuits that process the quantum information, and measurement operations that extract classical outputs. The parameters of the ansatz circuit are optimized iteratively using classical optimizers to minimize a cost function, enabling the circuit to learn patterns in the training data [26, 27].

Despite the theoretical promise of quantum machine learning, practical applications in blood cell analysis and hematological imaging have faced significant challenges. Previous studies applying quantum algorithms to blood cell classification and microscopic image analysis have consistently underperformed compared to state-of-the-art classical methods in hematology. While some quantum approaches have demonstrated improvements over basic classical baselines within their respective studies, these quantum methods have failed to achieve competitive performance compared to current best-practice classical techniques employed in modern deep learning architectures for blood cell identification and differential counting [28, 29]. The inability of previous quantum approaches to match classical performance in blood cell recognition tasks has limited their clinical relevance in automated hematology systems and hindered the translation of quantum computing advantages into practical benefits for blood-based diagnostics. Consequently, there remains an urgent need to develop quantum machine learning approaches specifically tailored for blood cell classification that can demonstrate competitive performance on hematologically relevant tasks, thereby establishing the viability of quantum computing in automated blood analysis and digital hematopathology.

The aim of this study is to develop an efficient and accurate blood cell classification model that addresses the computational limitations of traditional deep learning approaches. By integrating a variational quantum circuit (VQC) with a lightweight classical network, EfficientNet-B0, this study explores the potential of hybrid quantum-classical frameworks to enhance diagnostic accuracy while reducing computational overhead. This hybrid approach shows particular promise for deployment in resource-limited environments, where conventional deep learning methods would be suboptimal. Through this work, we aim to demonstrate that quantum-assisted models can serve as a viable alternative for medical image analysis, providing the foundation upon which more accessible and scalable diagnostic systems can be constructed. The key contributions of this study are as follows:

1. Design of a hybrid quantum-classical neural architecture that integrates variational quantum circuits with EfficientNet-based feature extraction for clinically relevant medical image classification tasks.
2. Demonstration of quantum-enhanced classification performance, achieving accuracy levels comparable to state-of-the-art classical models on standardized medical imaging benchmarks.
3. Comprehensive evaluation across all eight blood cell classes in the BloodMNIST dataset, establishing reproducible benchmarks for quantum-assisted haematological imaging.
4. Development of parameter-efficient quantum circuits, maintaining high classification accuracy while introducing minimal computational overhead.
5. Formulation of a stable and generalizable training strategy for hybrid quantum-classical models, optimized for medical image analysis under simulation-based quantum environments.
6. Validation of class-wise diagnostic reliability, demonstrating the model's suitability for potential integration into future automated haematology workflows.

The remainder of this paper is structured as follows: Section 2 reviews related work in classical and quantum machine learning approaches for blood cell classification. Section 3 presents the proposed methodology, including the BloodMNIST dataset description, EfficientNet-based feature extraction, quantum circuit design, and training configurations. Section 4 provides a comprehensive presentation of the experimental results, including performance metrics and detailed discussion of the findings. Finally, Section 5 concludes the paper and outlines future research directions in quantum-assisted medical image analysis.

2. RELATED WORKS

The related works section aims to explore existing methods used for blood cell classification, focusing particularly on deep learning (DL) techniques and their limitations. While DL models, such as convolutional neural networks and transfer learning frameworks, have shown impressive accuracy in medical image analysis, they often come with significant drawbacks. These include high computational requirements, long training times, and the need for large, annotated datasets—factors that make deployment challenging, especially in low-resource clinical settings. Moreover, the black-box nature of many DL models raises concerns about interpretability and trust in medical decision-making. This section also reviews emerging research on quantum and hybrid quantum-classical models, which are being investigated as potential solutions to address these challenges. By examining the progress and gaps in literature, the section lays the groundwork for the motivation and novelty of the proposed hybrid model in this study. Transfer learning approaches using pre-trained convolutional neural networks (CNNs) have been widely applied to blood cell classification tasks. According to Asghar et al. [30] evaluated eight pretrained CNN architectures (VGG16, VGG19, ResNet-50, ResNet-101, ResNet-152, InceptionV3, MobileNetV2 and DenseNet-201) across three datasets—PBC (17,092 images), Kaggle (12,500 images), and LISC (10,000 images)—to benchmark classification performance. They then developed a custom CNN architecture, trained from scratch without applying transfer learning, which achieved classification accuracies ranging from 98.79% to 99.91% across the datasets. While the paper does not explicitly address training efficiency, the absence of transfer learning suggests that the model may require longer training time and exhibit greater dependency on dataset size and quality, potentially affecting scalability in practical settings. Also study by Islam et al. [31] developed an enhanced convolutional neural network for four-class white blood cell classification, reporting a test accuracy of 99.12%, with 99% precision and an F1-score of 99%. The model was trained and evaluated on a dataset comprising 12,444 labelled images. It incorporated extensive image preprocessing steps—padding, thresholding, erosion, dilation, and masking—to reduce noise and highlight relevant cell morphology. Its architecture was optimized through experimentation with structural configurations and hyperparameters. Model explainability was addressed using SHAP, LIME, Grad-CAM, and Grad-CAM++ techniques, with Grad-CAM++ demonstrating slightly improved localization of diagnostic regions. However, the study was limited to four WBC classes and relied on complex preprocessing steps that may hinder generalizability. Another, Erten et al. [32] proposed ConcatNeXt, a CNN-based architecture that incorporates depth-concatenation mechanisms and patchify layers. The model was evaluated on the BloodMNIST dataset comprising 17,092 images across eight blood cell classes, achieving validation and test accuracies of 97.43% and 97.77%, respectively. Further improvements were obtained by applying a nested patch-based feature engineering pipeline, reaching an accuracy of 98.73%. While the performance results were promising, the dataset used primarily included white blood cell classes, limiting the representation of abnormal red blood cells.

Also, Toptaş et al. [33] proposed an ensemble CNN-based method for white blood cell classification, leveraging GoogLeNet, ResNet-50, and EfficientNet-B0 to extract features from the deep layers of each architecture. These features were concatenated and refined using the Minimum Redundancy Maximum Relevance (mRMR) algorithm to select the most informative 1500-dimensional feature subset. Classification was then performed using SVM and KNN classifiers. The method achieved an accuracy of 98.63% on a publicly available dataset comprising 12,444 images across four white blood cell types. Notably, the model did not require preprocessing or post-processing steps. However, the study lacked cross-dataset validation and was limited to only four WBC classes, raising concerns about its generalizability in broader clinical contexts.

Quantum machine learning (QML) applications in blood cell classification are still in their early stages. Singh et al. [29] proposed a fully quantum model for blood cell classification using 17,092 images from the MedMNIST dataset. Due to constraints associated with current NISQ hardware, the input images were substantially downsampled to 7×7 or 8×8, resulting in highly compressed feature representations (49 or 64 features). These features were angle-encoded into quantum states and processed through parameterized quantum circuits incorporating dynamical decoupling (DD) and measurement error mitigation (M3) techniques. Although the model operated entirely without classical neural layers, it achieved only 42.4% accuracy across eight blood cell classes. This performance gap is attributed to the aggressive input compression, the restricted expressivity of the quantum circuit, and residual quantum noise, all of which limit the model's capacity to capture class-specific patterns effectively. These findings underscore the current scalability and accuracy limitations of purely quantum approaches for complex image classification tasks such as blood cell analysis. A comparative analysis of existing blood cell classification models is summarized in Table 1, highlighting differences in architecture, datasets, and performance benchmarks across recent studies.

Table 1. Comparison of Blood Cell Classification Studies

Study / Year	Method	Dataset	Classes	Accuracy %	Limitations
Asghar et al. [30] 2024	Proposed CNN trained from scratch without transfer learning, after benchmarking eight pretrained CNNs	PBC (17,092), Kaggle-BCCD (12,500), LISC (10000)	10	98.79–99.91	Longer training time and higher dependency on dataset size and quality due to absence of transfer learning
Islam et al. [31] 2024	Enhanced CNN with extensive image preprocessing	WBC dataset (12,444 images)	4	99.12	Limited to four WBC classes, extensive preprocessing required
Erten et al. [32] 2025	CNN with depth concatenation blocks, patchify layer, nested patch-based deep feature engineering (SVM+NCA)	Custom (17,092 images)	8	98.73	Limited to white blood cell classes; abnormal red blood cells not included
Toptaş et al. [33] 2025	Ensemble CNNs + SVM	WBC dataset (12,444 images)	4	98.63	Limited cell types, single dataset validation
Singh et al. [29] 2025	Pure QML	BloodMNIST (17,092 images)	8	42.4	Feature compression required, quantum noise limitations

Current classical deep learning approaches achieve high accuracy in blood cell classification but remain limited by computational intensity and the need for large, well-annotated datasets. These factors constrain their applicability in low-resource settings. Moreover, many existing studies lack cross-dataset validation, raising concerns about generalizability across varying clinical imaging conditions. As classification complexity increases, classical architectures may also encounter scaling inefficiencies related to parameter growth and training time. For comparison, quantum machine learning methods remain in preliminary developmental stages. Standalone quantum models typically require aggressive dimensionality reduction due to current NISQ hardware limitations, which can result in loss of morphologically significant features. Additionally, hardware noise and limited circuit depth constrain performance on practical medical imaging tasks. These findings demonstrate the necessity of hybrid quantum-classical architectures that combine the representational efficiency of quantum encoding with the robustness of classical feature extractors. Such systems may offer computational advantages and improved scalability while addressing the inherent limitations of both standalone classical and quantum approaches.

3. THE PROSED METHODOLOGY

This section describes the overall methodology used to design and evaluate the hybrid quantum-classical neural network for classifying blood cells. The methodology tries to achieve hybrid quantum-classical system between accuracy and computational cost for blood cell classification. The methodology uses the hybrid of a 6-qubit variational quantum circuit (VQC) and the EfficientNet-B0 deep network architecture to take advantage of quantum processing and lightweight convolution architectures. The process begins with preprocessing and normalization of the BloodMNIST dataset, followed by feature extraction using EfficientNet-B0. These extracted features are subsequently processed through the VQC, which is trained via quantum simulation to enhance learning capability while maintaining low resource consumption. The hybrid model is trained and evaluated using standard metrics, emphasizing high classification accuracy across all eight blood cell types. This methodology explores the integration of quantum computing into medical imaging while addressing the practical need for scalable and efficient diagnostic systems in healthcare. The proposed methodology is illustrated in Figure 1.

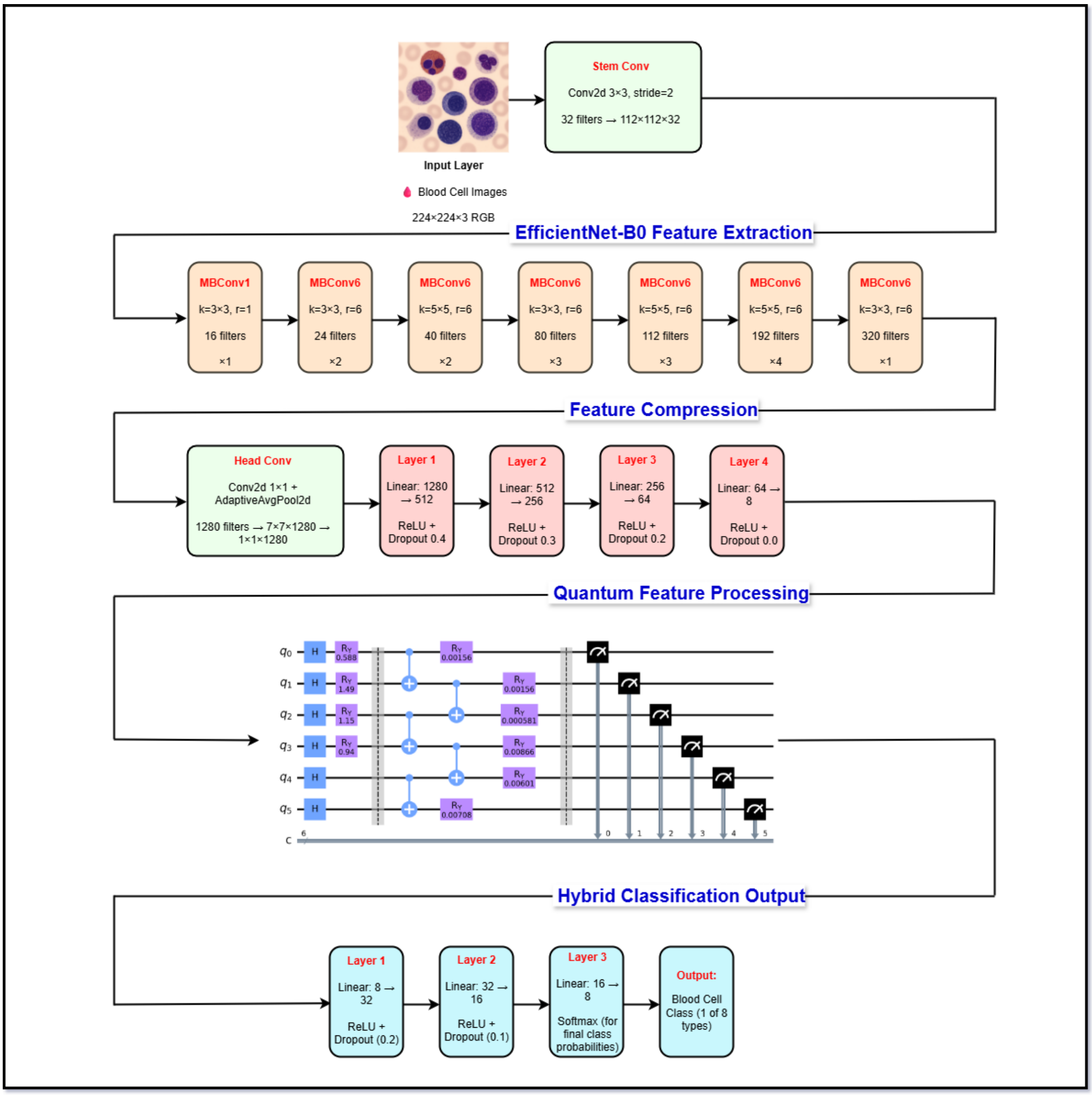

Figure 1: Proposed Hybrid Model for Blood Cell Image Classification

3.1 Dataset and Experimental Setup

This section describes the dataset characteristics, class distributions, and experimental configuration employed in this study. The methodology encompasses dataset selection, preprocessing protocols, and evaluation frameworks essential for reproducible research.

3.1.1 BloodMNIST Dataset

This study utilizes the BloodMNIST dataset, a standardized benchmark within the MedMNIST collection specifically designed for blood cell classification tasks. The dataset comprises 17,092 high-resolution RGB microscopic images representing eight distinct blood cell types commonly encountered in clinical hematology practice. The dataset is publicly available through the MedMNIST repository (https://medmnist.com/) [34].

The dataset follows a standard 70%-10%-20% train-validation-test split, yielding 11,959 training samples, 1,712 validation samples, and 3,421 test samples. The original images have a resolution of 28×28 pixels and are resized to 224×224 pixels during preprocessing to maintain compatibility with the pre-trained EfficientNet-B0 backbone. The eight blood cell classes represent physiologically relevant categories: basophils, eosinophils, erythroblasts, immature granulocytes, lymphocytes, monocytes, neutrophils, and platelets. Representative examples from each class are shown in Figure 2, while the dataset characteristics are summarized in Table 2.

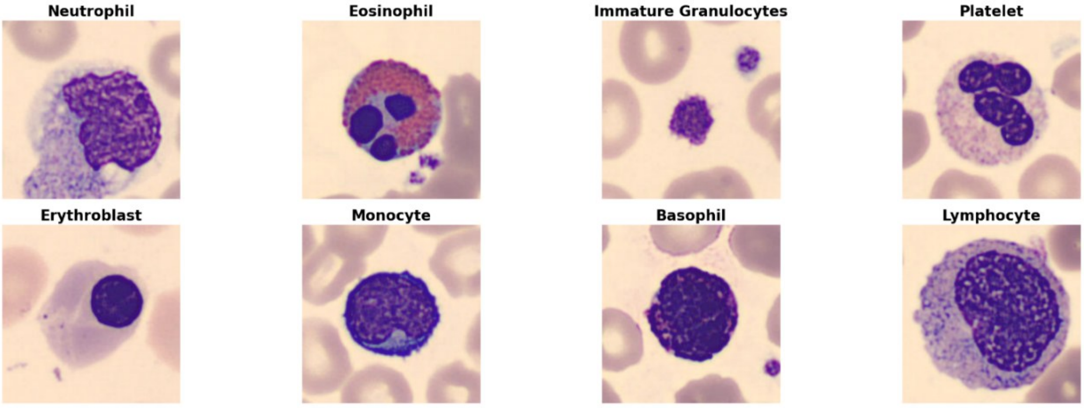

Figure 2: Example images from the BloodMNIST dataset across the eight blood cell classes

Table 2: Summary of BloodMNIST Dataset Characteristics

Attribute	Value
Total Images	17,092
Training Set	11,959 (70%)
Validation Set	1,712 (10%)
Test Set	3,421 (20%)
Original Resolution	28×28 pixels
Processed Resolution	224×224 pixels
Color Channels	RGB (3 channels)
Classes	Eight blood cell types

3.1.2 Class Distribution and Clinical Significance

The dataset exhibits natural class imbalance reflecting physiological blood cell distributions. Neutrophils constitute the largest class (19.5% of training samples), consistent with their prevalence in healthy blood, while basophils and lymphocytes represent smaller proportions (7.1% each). This imbalance necessitates specialized training strategies to ensure robust performance across all cell types. The complete class distribution and clinical significance of each cell type are presented in Table 3, while Figure 3 illustrates the proportional distribution graphically.

Table 3: Blood Cell Class Distribution and Clinical Significance

Cell Type	Training Samples	Clinical Role
Neutrophil	2,330	Bacterial defense
Eosinophil	2,181	Parasitic/allergic response
Immature Granulocytes	2,026	Immune activation
Platelet	1,643	Blood clotting
Erythroblast	1,085	Red blood cell production
Monocyte	993	Tissue repair
Basophil	852	Inflammatory response
Lymphocyte	849	Adaptive immunity

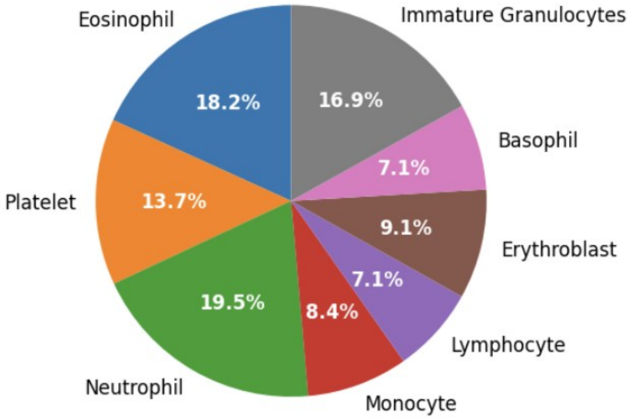

Figure 3: Class distribution of blood cells in the BloodMNIST training set

3.1.3 Data Preprocessing and Augmentation

The preprocessing pipeline standardizes input images while preserving morphological features essential for accurate blood cell classification. Normalization ensures compatibility with transfer learning from natural image domains, whereas augmentation strategies enhance robustness to imaging variability encountered in clinical settings.

All input images are normalized using ImageNet statistics (mean: $0.485, 0.456, 0.406$; standard deviation: $0.229, 0.224, 0.225$), enabling effective reuse of pretrained weights in the EfficientNet-BO backbone. This step promotes feature consistency across domains and improves generalization performance.

To simulate realistic blood smear preparation conditions, the training set is augmented using random resized cropping (scale: $0.8-1.0$), horizontal and vertical flips, and rotations within $\pm 15^{\circ}$. These transformations account for variability in microscope magnification, slide orientation, and sample alignment. Additional photometric augmentations-including adjustments to brightness, contrast, saturation, and hue-simulate staining protocol variability across laboratory environments.

To address class imbalance in the training set, class weights were computed proportionally to balance the contribution of each blood cell type during training. This strategy ensures that minority classes receive proportionally greater emphasis during optimization, enhancing classification performance across underrepresented categories such as lymphocytes and basophils.

3.2 Model Architecture

This section presents the overall structure of the hybrid quantum-classical model designed for blood cell classification. The architecture consists of three main modules:

(1) a classical feature extractor based on EfficientNet-B0,
(2) a dimensionality reduction network, and
(3) a quantum variational circuit for enhanced feature transformation.

These components form a unified, end-to-end trainable pipeline that integrates classical and quantum computations to optimize diagnostic accuracy while maintaining efficiency.

3.2.1 Classical Feature Extraction and Processing

EfficientNet-B0 is used as the classical backbone for feature extraction due to its high accuracy-to-complexity ratio. Pre-trained on ImageNet [35], the model includes 4,007,548 parameters. Its final classification head is removed to expose a 1,280-dimensional feature embedding per input image. This embedding captures high-level morphological characteristics relevant for distinguishing between blood cell types.

To prepare features for quantum processing, a four-layer Multi-Layer Perceptron (MLP) is used to compress the 1,280-dimensional output into eight features. Each layer applies a linear transformation, batch normalization, ReLU activation, and dropout regularization with decreasing dropout rates of 0.4, 0.3, 0.2, and 0.0. This step ensures information preservation while reducing dimensionality. The full architecture is summarized in Table 4.

Table 4: Feature Processing Network Architecture

Layer	Input Dim	Output Dim	Activation	Dropout Rate
Layer 1	1280	512	ReLU	0.4
Layer 2	512	256	ReLU	0.3
Layer 3	256	64	ReLU	0.2
Layer 4	64	8	ReLU	0.0

3.2.2 Quantum Network Architecture

The quantum module implements a six-qubit variational quantum circuit (VQC) composed of four trainable layers. The input interface encodes four classical features into the amplitudes of four dedicated qubits using angle embedding. Two additional qubits are reserved to enhance entanglement and capture complex correlations during quantum state evolution.

The circuit follows a layered structure with alternating entanglement and rotation blocks. Even-numbered layers apply CNOT entanglement between qubit pairs (0,1), (2,3), and (4,5), while odd-numbered layers entangle (1,2) and (3,4). Parameterized RY rotations are applied across all qubits within each layer, enabling expressive quantum transformations. After final measurements, six expectation values are extracted and mapped to an 8-dimensional classical vector through a linear post-processing layer. The complete quantum circuit is shown in Figure 4.

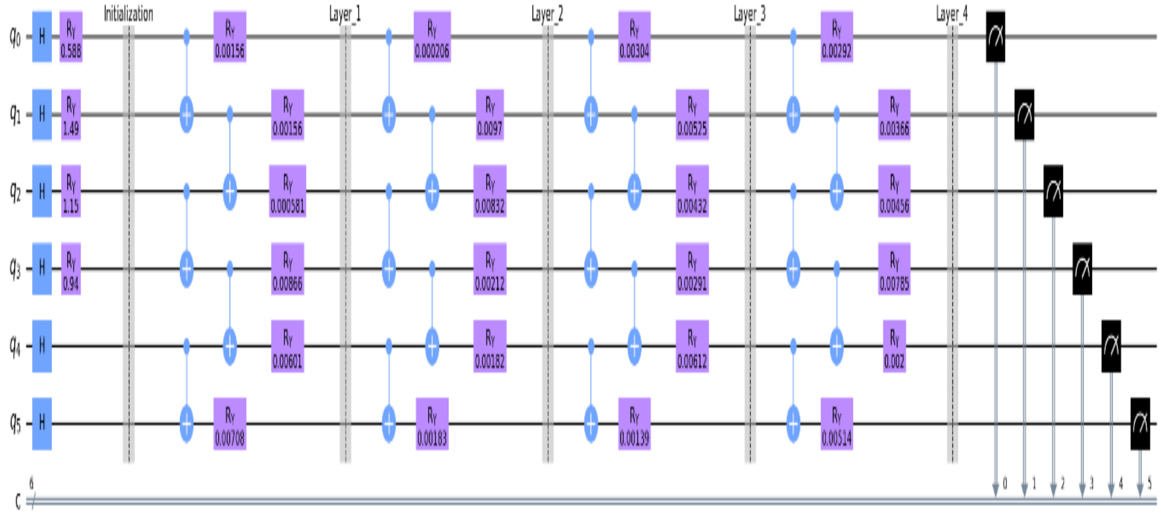

Figure 4: Variational quantum circuit architecture with six qubits, four parameterized layers, and angle embedding.

3.2.3 Final Classification Layer

The 8-dimensional quantum-enhanced feature vector is passed to a fully connected neural classifier composed of three dense layers. This module transforms the processed features into a probability distribution across the eight target blood cell classes. The classifier is trained jointly with all previous components, allowing gradient propagation through the quantum layer to optimize the entire pipeline in an end-to-end fashion.

3.3 Training Strategy and Optimization

The hybrid model was trained end-to-end using the AdamW optimizer [36], with differentiated learning rates assigned to each model component. The EfficientNet-B0 backbone was updated conservatively (3×10^{-5}) to retain pre-trained knowledge, quantum parameters used a higher rate (5×10^{-3}) to facilitate fast convergence, and intermediate classical layers adopted a moderate rate (1×10^{-3}). Training regularization included label smoothing cross-entropy loss ($\varepsilon = 0.1$) with inverse frequency weighting, and global gradient clipping (max-norm = 1.0) to ensure numerical stability across the hybrid architecture. These strategies contributed to balanced learning across the quantum and classical subsystems.

3.4 Experimental Configuration

Model training was conducted using a CUDA-enabled GPU, with quantum circuit simulation handled via PennyLane. The configuration employed a batch size of 32, optimized to balance GPU memory usage and gradient stability. Training was conducted for 100 epochs without early stopping, allowing full convergence of both classical and quantum components. The evaluation protocol incorporated a diverse set of performance metrics including overall accuracy, per-class precision and recall, macro and weighted F1-scores, Cohen's Kappa coefficient, and ROC-AUC curves. This multi-dimensional strategy ensures rigorous and clinically meaningful performance assessment across all eight blood cell categories, with implementation details presented in Algorithm 1.

Algorithm 1 Hybrid Quantum-Classical Blood Cell Classification

```
Require: BloodMNIST dataset $D = \{(x_i, y_i)\}_{i=1}^{17092}$, where $x_i \in \mathbb{R}^{224\times224\times3}$,
    $y_i \in \{0, 1, \ldots, 7\}$
Ensure: Trained hybrid model $\theta^*$
Data Preparation:
    Load BloodMNIST: 70% train, 10% validation, 20% test
    Apply augmentation: rotation, flip, color jitter
    Normalize with ImageNet statistics
Hybrid Model Architecture:
    Classical backbone: EfficientNet-B0 $\rightarrow$ 1,280 features
    Feature processor: 4-layer MLP $(1,280 \rightarrow 8)$
    Quantum layer: 6-qubit VQC with 24 parameters
    Final classifier: 3-layer MLP $(8 \rightarrow 8)$
Quantum Circuit (6-qubit VQC):
    Initialize: Apply Hadamard gates to all qubits
    Encode: First 4 features using RY rotations
    Parameterized layers $(\times 4)$: RY rotations + CNOT entanglement
    Measure: PauliZ expectations $\rightarrow$ 6 quantum features
Training Procedure:
    Loss: Label smoothing cross-entropy $(\epsilon = 0.1)$
    Optimizer: AdamW with differential learning rates
        Backbone: $3 \times 10^{-5}$, Quantum: $5 \times 10^{-3}$, Others: $1 \times 10^{-3}$
    Regularization: Gradient clipping, dropout, batch normalization
    Schedule: ReduceLROnPlateau, 100 epochs
Evaluation:
    Compute test accuracy and validation accuracy
    Calculate precision, recall, F1-scores per class
    Generate confusion matrix and performance metrics
return Trained model $\theta^*$, performance metrics
```

4. RESULTS AND DISCUSSION

This section delineates the experimental findings of the hybrid quantum-classical model and analyzes their implications for blood cell classification and clinical applications. The results are discussed in the context of existing literature and clinical requirements to provide comprehensive insights into model performance and practical deployment considerations.

4.1 Model Performance and Training Dynamics

The hybrid quantum-classical model achieved 96.58% test accuracy after 100 epochs of training, with peak validation performance of 97.20% at epoch 61. The training progression over 1,386 minutes, illustrated in Figure 5, demonstrates steady convergence without overfitting. The close alignment between validation and test performance indicates robust learning and generalization stability essential for medical applications.

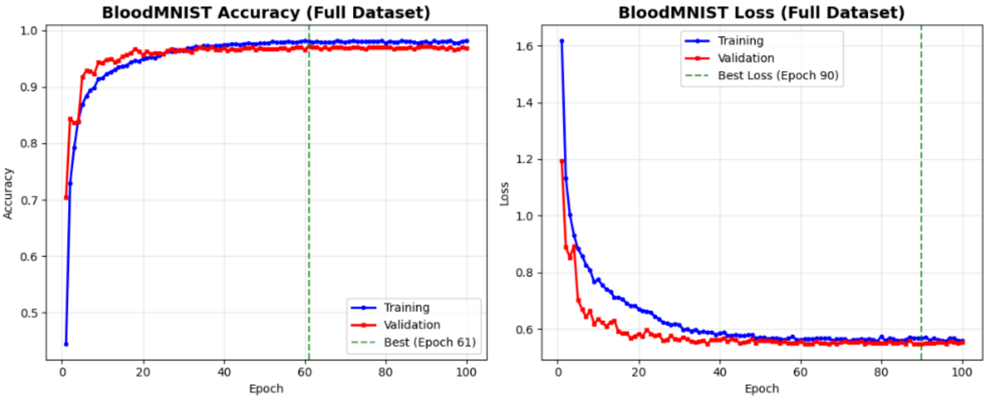

Figure 5: Training Performance Curves

Table 5 summarizes the performance across all dataset splits, confirming the consistent results observed in the training curves.

Table 5: Model Performance Summary

Dataset Split	Samples	Accuracy	Macro F1	Weighted F1	Cohen's Kappa
Training	11,936	99.11%	99.12%	99.11%	99.05%
Validation	1,712	96.90%	96.69%	96.87%	96.39%
Test	3,421	96.58%	96.52%	96.65%	96.15%

4.2 Per-Class Analysis and Clinical Implications

Table 6 presents the per-class performance metrics, revealing varied accuracy levels across different blood cell types that reflect their morphological complexity and clinical significance.

Table 6: Per-Class Performance Analysis

Cell Type	Samples	Precision %	Recall %	F1-Score %	Accuracy %
Eosinophil	312	100.00	99.68	99.84	99.68
Platelet	235	100.00	99.15	99.57	99.15
Neutrophil	333	96.20	98.80	97.48	98.80
Monocyte	143	96.55	97.90	97.22	97.90
Lymphocyte	122	95.24	98.36	96.77	98.36
Erythroblast	155	93.37	100.00	96.57	100.00
Basophil	122	90.84	97.54	94.07	97.54
Immature Granulocytes	290	97.67	86.90	91.97	86.90

As illustrated in Figure 6, Eosinophils and platelets achieved the highest accuracy levels, likely due to their distinctive morphological features. Eosinophils possess characteristic orange-red granules that provide clear visual markers, while platelets appear as distinct cellular fragments. The strong performance on neutrophils (98.80% accuracy) and lymphocytes (98.36% accuracy) is clinically significant, as these cells serve as primary indicators for bacterial infections and immune system status respectively.

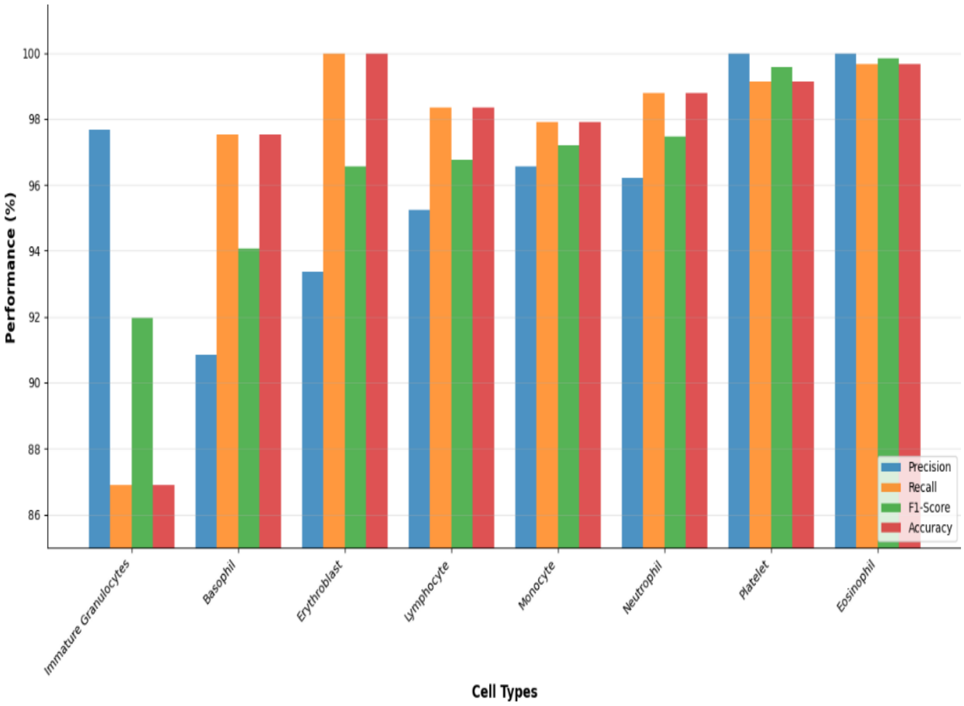

Figure 6: Per-Class Performance Comparison

Immature granulocytes presented the greatest classification challenge with 86.90% accuracy. This cell category encompasses multiple developmental stages with overlapping morphological characteristics, making accurate discrimination inherently difficult. The confusion matrix analysis (Figure 7) shows that most errors occur between morphologically similar cell types, particularly immature granulocytes being misclassified as basophils (11 cases), which represents a clinically understandable error given their shared granulocytic lineage.

True \ Predicted	basophil	eosinophil	erythrobla..	immature g..	lymphocyte	monocyte	neutrophil	platelet
basophil	119 (97.5%)	0 (0.0%)	0 (0.0%)	1 (0.8%)	2 (1.6%)	0 (0.0%)	0 (0.0%)	0 (0.0%)
eosinophil	0 (0.0%)	311 (99.7%)	0 (0.0%)	0 (0.0%)	0 (0.0%)	0 (0.0%)	1 (0.3%)	0 (0.0%)
erythrobla..	0 (0.0%)	0 (0.0%)	155 (100.0%)	0 (0.0%)	0 (0.0%)	0 (0.0%)	0 (0.0%)	0 (0.0%)
immature g..	11 (3.8%)	0 (0.0%)	9 (3.1%)	252 (86.9%)	3 (1.0%)	4 (1.4%)	11 (3.8%)	0 (0.0%)
lymphocyte	1 (0.8%)	0 (0.0%)	0 (0.0%)	1 (0.8%)	120 (98.4%)	0 (0.0%)	0 (0.0%)	0 (0.0%)
monocyte	0 (0.0%)	0 (0.0%)	0 (0.0%)	1 (0.7%)	1 (0.7%)	140 (97.9%)	1 (0.7%)	0 (0.0%)
neutrophil	0 (0.0%)	0 (0.0%)	0 (0.0%)	3 (0.9%)	0 (0.0%)	1 (0.3%)	329 (98.8%)	0 (0.0%)
platelet	0 (0.0%)	0 (0.0%)	2 (0.9%)	0 (0.0%)	0 (0.0%)	0 (0.0%)	0 (0.0%)	233 (99.1%)

Figure 7: Confusion Matrix Analysis

4.3 Quantum Component Efficiency and Impact

The quantum component demonstrated exceptional parameter efficiency, achieving a test accuracy of 96.58% using only 24 trainable parameters. Despite this minimal configuration, it had a tangible impact on classification performance. The quantum circuit's ability to process four classical features and generate six measurement outputs indicates that quantum transformations can encode complex feature relationships that are not easily replicated through classical models of comparable size.

When compared to equivalent classical architectures with similar parameter budgets, the quantum design leverages the 64-dimensional quantum state space (2^6 qubits) to perform expressive transformations that would require substantially more classical resources to approximate. This advantage offers practical implications for deployment in resource-constrained environments or scenarios where quantum hardware access offers computational or cost-related benefits over classical scaling.

4.4 Comparative Performance Analysis

Table 7 summarizes the test accuracies of recent deep learning and quantum-enhanced models for blood cell classification. The proposed hybrid quantum-classical model achieved an accuracy of 96.58% on the full 8-class BloodMNIST dataset. Compared to Erten et al. [32], which reported 97.77% on the same dataset, the modest 1.19% performance gap reflects a justifiable compromise given the model's improved parameter efficiency and compatibility with near-term quantum hardware.

Notably, the hybrid architecture substantially outperforms the fully quantum method introduced by Singh et al. [29], which reached only 42.4% accuracy. This disparity underscores the challenges faced by quantum-only approaches, particularly when constrained by aggressive input compression, circuit depth limitations, and quantum noise. By combining robust classical feature extraction with a quantum variational layer, the proposed method achieves a more balanced and scalable solution, better suited to the capabilities of current NISQ-era systems.

Table 7: Performance Comparison Summary

Study	Dataset Used	Test Accuracy %
Islam et al. (2024) [31]	WBC Dataset (4 classes)	99.12
Erten et al. (2025) [32]	BloodMNIST (8 classes)	97.77
Singh et al. (2025) [29]	BloodMNIST (8 classes)	42.4
Toptaş et al. (2025) [33]	WBC Dataset (4 classes)	98.63
The proposed Work	**BloodMNIST (8 classes)**	**96.58**

4.5 Clinical Deployment Considerations

The model demonstrates operational readiness for integration into high-throughput clinical workflows. The 96.58% accuracy meets the typical performance thresholds required by automated haematology analyzers, which often demand accuracy exceeding 95% for routine diagnostic tasks. Cohen's Kappa score of 96.39% further supports strong agreement with expert annotations, aligning with levels suitable for clinical validation. Nevertheless, several challenges remain before practical deployment. The current implementation operates under quantum simulation rather than real quantum hardware, potentially leading to performance discrepancies due to noise and decoherence when deployed on physical devices. Moreover, the limited interpretability of quantum components poses a barrier to clinical acceptance, where transparency in diagnostic decision-making is critical for patient safety.

4.6 Limitations and Future Directions

The evaluation is limited to a single standardized dataset, which may not fully represent the morphological diversity encountered across different clinical settings and patient populations. Future validation should include diverse clinical cohorts and conducting multi-institutional studies to establish broader generalizability. The quantum circuit implementation currently relies on simulation rather than actual quantum hardware execution. Real quantum devices introduce noise and gate fidelity limitations that may affect performance. Future work should investigate noise-resilient circuit designs and evaluate performance on actual quantum hardware platforms. The hybrid architecture's scalability presents both opportunities and challenges. While the current 6-qubit implementation demonstrates proof-of-concept viability, larger quantum circuits may enable more complex medical imaging tasks. However, scaling must be balanced against current quantum hardware limitations and practical deployment considerations including infrastructure requirements and cost-effectiveness compared to classical alternatives.

5. CONCLUSION

This study introduced a hybrid quantum–classical model for blood cell classification, integrating EfficientNet-B0 as a classical feature extractor with a six-qubit variational quantum circuit to enhance decision-making. The proposed architecture successfully leverages quantum encoding and entanglement to enrich feature representation while remaining fully compatible with classical deep learning pipelines. Dimensionality reduction prior to quantum processing mitigated the limitations of NISQ hardware, enabling efficient angle encoding with minimal information loss. Experimental evaluation across eight blood cell classes using the BloodMNIST dataset yielded strong results, with a test accuracy of 96.58% and F1-scores ranging from 91.97% to 99.84%, confirming the model’s robustness and practical diagnostic relevance. These outcomes highlight the feasibility of integrating quantum computation into real-world biomedical imaging tasks. For the future research may benefit from implementing the model on real quantum hardware to assess performance under realistic noise conditions. Moreover, exploring adaptive variational circuits that scale with data complexity and patient variability could enhance flexibility. Finally, expanding the framework to incorporate multimodal medical data, such as genomic or clinical metadata, holds promise for building more comprehensive and accurate diagnostic systems.

FUNDING INFORMATION

This research did not receive any specific grant from funding agencies in the public, commercial, or not-for-profit sectors.

COFLICTS OF INTERESTS

The authors declare that there is no conflict of interest regarding the publication of this paper.

DATA AVAILABILITY STATEMENTS

The dataset used in this study is publicly available at the following link: https://medmnist.com/

DECLARATION OF GENERATIVE AI AND AI-ASSISTED TECHNOLOGIES IN THE WRITING PROCESS

During the preparation of this work, the authors used ChatGPT (OpenAI) to improve the clarity and readability of the manuscript. After using this tool, the authors reviewed and edited the content as needed and take full responsibility for the content of the publication.

REFERENCES

[1] J. El Brihi and S. Pathak, "Normal and Abnormal Complete Blood Count With Differential," in *StatPearls*. Treasure Island (FL), 2025.

[2] A. Shah, S. Srivastava, and C. P. Chaturvedi, "Biomolecular Components of Blood and Their Role in Health and Diseases," in *Clinical Applications of Biomolecules in Disease Diagnosis: A Comprehensive Guide to Biochemistry and Metabolism*, R. L. Singh, P. Singh, and N. Pathak Eds. Singapore: Springer Nature Singapore, 2024, pp. 289-322.

[3] B. George-Gay and K. Parker, "Understanding the complete blood count with differential," *Journal of PeriAnesthesia Nursing,* vol. 18, no. 2, pp. 96-117, 2003/04/01/ 2003, doi: https://doi.org/10.1053/jpan.2003.50013.

[4] M. Daves *et al.*, "Modern hematology analyzers: beyond the simple blood cells count (with focus on the red blood cells)," *Journal of Laboratory and Precision Medicine,* vol. 9, 2023. [Online]. Available: https://jlpm.amegroups.org/article/view/8320.

[5] A. Gautam and H. Bhadauria, "Classification of white blood cells based on morphological features," in *2014 International Conference on Advances in Computing, Communications and Informatics (ICACCI)*, 24-27 Sept. 2014 2014, pp. 2363-2368, doi: 10.1109/ICACCI.2014.6968362.

[6] C. Rosales, "Neutrophils at the crossroads of innate and adaptive immunity," *Journal of Leukocyte Biology,* vol. 108, no. 1, pp. 377-396, 2020, doi: 10.1002/jlb.4mir0220-574rr.

[7] K. A. Radhi, I. H. Hamzah, and B. F. Matti, "The role of miRNA -181C between different BCR-ABL p210 transcript levels and between different levels of imatinib optimal response in CML patients," *Human Gene,* Article vol. 34, 2022, Art no. 201128, doi: 10.1016/j.humgen.2022.201128.

[8] A. Kratz, S. H. Lee, G. Zini, J. A. Riedl, M. Hur, and S. Machin, "Digital morphology analyzers in hematology: ICSH review and recommendations," (in eng), *Int J Lab Hematol,* vol. 41, no. 4, pp. 437-447, Aug 2019, doi: 10.1111/ijlh.13042.

[9] W. Cheng, J. Liu, C. Wang, R. Jiang, M. Jiang, and F. Kong, "Application of image recognition technology in pathological diagnosis of blood smears," (in eng), *Clin Exp Med,* vol. 24, no. 1, p. 181, Aug 6 2024, doi: 10.1007/s10238-024-01379-z.

[10] Y. M. Kobara, I. J. Akpan, A. D. Nam, F. H. AlMukthar, and M. Peter, "Artificial Intelligence and Data Science Methods for Automatic Detection of White Blood Cells in Images," *Journal of Imaging Informatics in Medicine,* 2025/05/16 2025, doi: 10.1007/s10278-025-01538-y.

[11] H. Sazak and M. Kotan, "Automated Blood Cell Detection and Classification in Microscopic Images Using YOLOv11 and Optimized Weights," *Diagnostics,* vol. 15, no. 1, p. 22, 2025. [Online]. Available: https://www.mdpi.com/2075-4418/15/1/22.

[12] M. Ilyas, M. Bilal, N. Malik, H. U. Khan, M. Ramzan, and A. Naz, "Using Deep Learning Techniques to Enhance Blood Cell Detection in Patients with Leukemia," *Information,* vol. 15, no. 12, p. 787, 2024. [Online]. Available: https://www.mdpi.com/2078-2489/15/12/787.

[13] M. Abou Ali, F. Dornaika, and I. Arganda-Carreras, "White Blood Cell Classification: Convolutional Neural Network (CNN) and Vision Transformer (ViT) under Medical Microscope," *Algorithms,* vol. 16, no. 11, p. 525, 2023. [Online]. Available: https://www.mdpi.com/1999-4893/16/11/525.

[14] S. Choudhary *et al.*, "Advancing blood cell detection and classification: performance evaluation of modern deep learning models," *BMC Medical Informatics and Decision Making,* vol. 25, no. 1, p. 207, 2025/06/04 2025, doi: 10.1186/s12911-025-03027-2.

[15] L. Wei *et al.*, "Quantum machine learning in medical image analysis: A survey," *Neurocomputing,* vol. 525, pp. 42-53, 2023/03/07/ 2023, doi: https://doi.org/10.1016/j.neucom.2023.01.049.

[16] B. Subbiyan, R. P. Neelakandan, K. Leelasankar, R. Rajavel, M. Malarvel, and A. Shankar, "A Quantum-Enhanced Artificial Neural Network Model for Efficient Medical Image Compression," *IEEE Access,* vol. 13, pp. 31809-31828, 2025, doi: 10.1109/ACCESS.2025.3542807.

[17] E. A. Radhi, M. Y. Kamil, and M. A. Mohammed, "Quantum Machine and Deep Learning for Medical Image Classification: A Systematic Review of Trends, Methodologies, and Future Directions," *Iraqi Journal for Computer Science and Mathematics,* Review vol. 6, no. 2, pp. 107-138, 2025, doi: 10.52866/2788-7421.1252.

[18] T. Torda, "Interpretability and explainability AI in advanced neural Networks for topological quantum field Theory and medical application," 2024.

[19] F. F. Flöther, "The state of quantum computing applications in health and medicine," *Research Directions: Quantum Technologies,* vol. 1, p. e10, 2023, Art no. e10, doi: 10.1017/qut.2023.4.

[20] R. Anuradha, C. Vandana, S. V. Singh, N. Singh, R. Emad, and V. Nitin, "Integrating Quantum Computing for Enhanced Image Reconstruction in Medical Diagnostics," in *2024 International Conference on Communication, Computer Sciences and Engineering (IC3SE)*, 2024: IEEE, pp. 1294-1298.

[21] S.-S. Ahmadpour, D. B. Avval, M. Darbandi, N. J. Navimipour, N. U. Ain, and S. Kassa, "A new quantum-enhanced approach to AI-driven medical imaging system," *Cluster Computing,* vol. 28, no. 3, p. 213, 2025/01/28 2025, doi: 10.1007/s10586-024-04852-2.

[22] P. LAMICHHANE and D. B. RAWAT, "Quantum Machine Learning: Recent Advances, Challenges, and Perspectives," 2025.

[23] A. Marengo and V. Santamato, "Quantum algorithms and complexity in healthcare applications: a systematic review with machine learning-optimized analysis," (in English), *Frontiers in Computer Science,* Review vol. Volume 7 - 2025, 2025-May-07 2025, doi: 10.3389/fcomp.2025.1584114.

[24] Y. Wang and J. Liu, "A comprehensive review of quantum machine learning: from nisq to fault tolerance," *Reports on Progress in Physics,* 2024.

[25] Y. Gujju, A. Matsuo, and R. Raymond, "Quantum machine learning on near-term quantum devices: Current state of supervised and unsupervised techniques for real-world applications," *Physical Review Applied,* vol. 21, no. 6, p. 067001, 2024.

[26] S. An and K. Slavakis, "Tensor-Based Binary Graph Encoding for Variational Quantum Classifiers," in *2025 International Conference on Quantum Communications, Networking, and Computing (QCNC)*, 2025: IEEE, pp. 568-574.

[27] A. Regadío, "Exoplanet discovery with variational quantum circuits," *Quantum Machine Intelligence,* vol. 7, no. 1, p. 11, 2025.

[28] C.-S. Chen, "Vision-QRWKV: Exploring Quantum-Enhanced RWKV Models for Image Classification," *arXiv preprint arXiv:2506.06633,* 2025.

[29] G. Singh, H. Jin, and K. M. Merz Jr, "Benchmarking MedMNIST dataset on real quantum hardware," *arXiv preprint arXiv:2502.13056,* 2025.

[30] R. Asghar, S. Kumar, and P. Hynds, "Automatic classification of 10 blood cell subtypes using transfer learning via pre-trained convolutional neural networks," *Informatics in Medicine Unlocked,* vol. 49, p. 101542, 2024.

[31] O. Islam, M. Assaduzzaman, and M. Z. Hasan, "An explainable AI-based blood cell classification using optimized convolutional neural network," *Journal of Pathology Informatics,* vol. 15, p. 100389, 2024.

[32] M. Erten, P. D. Barua, S. Dogan, T. Tuncer, R.-S. Tan, and U. Acharya, "ConcatNeXt: An automated blood cell classification with a new deep convolutional neural network," *Multimedia Tools and Applications,* pp. 1-19, 2024.

[33] M. Toptaş, B. Toptaş, and D. Hanbay, "Classifying white blood cells using combining different convolutional neural networks," *Multimedia Tools and Applications,* 2025/05/08 2025, doi: 10.1007/s11042-025-20879-y.

[34] J. Yang *et al.*, "MedMNIST v2 - A large-scale lightweight benchmark for 2D and 3D biomedical image classification," *Scientific Data,* vol. 10, no. 1, p. 41, 2023/01/19 2023, doi: 10.1038/s41597-022-01721-8.

[35] M. Tan and Q. Le, "EfficientNet: Rethinking Model Scaling for Convolutional Neural Networks," presented at the Proceedings of the 36th International Conference on Machine Learning, Proceedings of Machine Learning Research, 2019. [Online]. Available: https://proceedings.mlr.press/v97/tan19a.html.

[36] I. Loshchilov and F. Hutter, "Fixing Weight Decay Regularization in Adam," *ArXiv,* vol. abs/1711.05101, 2017.